PHYSICAL REVIEW B **87**, 115146 (2013)

Kohn-Sham density functional theory for quantum wires in arbitrary correlation regimes

Francesc Malet,[1] André Mirtschink,[1] Jonas C. Cremon,[2] Stephanie M. Reimann,[2] and Paola Gori-Giorgi[1]

[1]*Department of Theoretical Chemistry and Amsterdam Center for Multiscale Modeling, FEW, Vrije Universiteit, De Boelelaan 1083, 1081HV Amsterdam, The Netherlands*

[2]*Mathematical Physics, Lund University, LTH, P. O. Box 118, SE-22100 Lund, Sweden*

(Received 30 January 2013; published 28 March 2013)

We use the exact strong-interaction limit of the Hohenberg-Kohn energy density functional to construct an approximation for the exchange-correlation term of the Kohn-Sham approach. The resulting exchange-correlation potential is able to capture the features of the strongly correlated regime without breaking the spin or any other symmetry. In particular, it shows "bumps" (or barriers) that give rise to charge localization at low densities and that are a well-known key feature of the exact Kohn-Sham potential for strongly correlated systems. Here, we illustrate this approach for the study of both weakly and strongly correlated model quantum wires, comparing our results with those obtained with the configuration interaction method and with the usual Kohn-Sham local density approximation.

DOI: 10.1103/PhysRevB.87.115146 PACS number(s): 71.15.Mb, 31.15.ec, 73.21.Hb

I. INTRODUCTION

In semiconductor nanostructures, the regime of strong correlation is reached when the electronic density becomes low enough so that the Coulomb repulsion becomes dominant with respect to the kinetic energy of the electrons. From the purely fundamental point of view, the study of the strongly interacting limit in such systems is interesting since charge localization, reminiscent of the Wigner crystallization[1] of the bulk electron gas, is expected to occur at low densities.

A lot of previous theoretical work on Wigner localization in nanostructures has focused on finite-sized quantum dots (see, for example, Refs. 2–7), and the crossover from liquid to localized states in the transport properties of the nanostructure has been addressed.[8,9] In quasi-one-dimensional nanosystems, signatures of Wigner localization were observed experimentally in one-dimensional (1D) cleaved-edge overgrowth structures,[10] or in the transport properties of InSb nanowire quantum-dot systems.[11] More recent experimental work clearly identified the formation of Wigner molecules in a one-dimensional quantum dot that was capacitively coupled to an atomic force microscope probe.[12] Wigner localization has also been investigated in other 1D systems such as carbon nanotubes.[13–15] (For a review, see Ref. 16.) Finally, regarding practical applications, Wigner-localized systems have been shown to be potentially useful, e.g., for quantum-computing purposes.[13,17]

When trying to model electronic strongly correlated systems, however, the commonly employed methodologies encounter serious difficulties of a different nature. On the one hand, the configuration interaction (CI) approach, despite being in principle capable of describing any correlation regime, is in practice limited to the study of small systems with only very few particles due to its high computational cost, which scales exponentially with the number of particles N. Such numerical difficulties get even worse in the very strongly correlated limit due to the degeneracy of the different quantum states and the consequent need of considering larger Hilbert spaces in the calculations. Other wave-function methods such as quantum Monte Carlo[7,18–20] (QMC) and density matrix renormalization group (DMRG),[21] which rely to some extent on various approximations, can treat systems larger than the CI approach, but are still computationally expensive and limited to $N \lesssim 10^2$.

The much cheaper Kohn-Sham (KS) density functional theory (DFT),[22,23] which can treat thousands of electrons, is the method of choice to study larger quantum systems. However, all the currently available approximations for the exchange-correlation functional fail to describe the strongly correlated regime[7,24–28] even at the qualitative level. Allowing spin- and spatial-symmetry breaking may yield reasonable total energies, without, however, capturing the physics of charge localization in nonmagnetic systems. Moreover, broken-symmetry solutions often yield a wrong characterization of various properties and the rigorous KS-DFT framework is partially lost (see, e.g., Refs. 21, 24, and 27).

KS DFT is, in principle, an exact theory that should be able to yield the exact energy and density even in the case of strong electronic correlation, without artificially breaking any symmetry. However, when dealing with practical KS DFT, one could expect that the noninteracting reference system introduced by Kohn and Sham might not be the best choice when trying to address systems in which the electron-electron interactions play a dominant role. For many years, huge efforts have been made in order to try to get a better characterization and understanding of the properties of the exact Kohn-Sham reference system (see, e.g., Refs. 21, 26, and 29–45). All these works reflected the large difficulties encountered when trying to obtain adequate approximations to describe strong correlation in the exact KS theory.[46]

An alternative density functional framework, based on the study of the strongly interacting limit of the Hohenberg-Kohn (HK) density functional, was presented in Ref. 47. In this approach, a reference system with infinite correlation between the electrons was considered instead of the noninteracting one of Kohn and Sham. The two formalisms can therefore be seen as complementary to each other and, indeed, the first results obtained with this so-called strictly correlated-electrons (SCE) DFT, presently limited to either 1D or spherically symmetric systems, showed its ability to describe systems in the extreme strongly correlated regime with a much better accuracy than

standard KS DFT.[47,48] On the downside, however, SCE DFT requires that one knows *a priori* that the system is in the strong-interaction regime, and it fails as soon as the fermionic nature of the electrons plays a significant role.[48] Furthermore, the formalism lacks some of the appealing properties of the Kohn-Sham approach, such as its capability to predict (at least in principle) exact ionization energies. Also, crucial concepts widely employed in solid state physics and in chemistry, such as the Kohn-Sham orbitals and orbital energies, are totally absent in SCE DFT.

Very recently, a new approach that combines the advantages of the KS and the SCE-DFT formalisms, consisting in approximating the Kohn-Sham exchange-correlation energy functional with the strong-interaction limit of the Hohenberg-Kohn energy density functional, has been proposed.[49] Pilot tests of this new "KS-SCE" framework showed that it is able to capture the features of both the weakly and the strongly correlated regimes in semiconductor quantum wires, as well as the so-called $2k_F \to 4k_F$ crossover occurring in-between them, while keeping (at least for 1D systems) a computational cost comparable to the one of standard KS DFT with the local-density approximation (LDA). In other words, the SCE functional yields a highly nonlocal approximation for the exchange-correlation energy functional, which is able to capture key features of strong correlation within the KS scheme, without any artificial symmetry breaking.

The main purpose of this work is to further investigate this new KS-SCE method by discussing its exact formal properties and, for the prototypical case of (quasi)-1D quantum wires, by also performing full CI calculations to compare electronic densities, total energies, and one-electron removal energies in different regimes of correlation. We find that the KS-SCE results are qualitatively right at all correlation regimes, representing an important advance for KS DFT. However, while one-electron removal energies are quite accurate, total energies and ground-state densities are still quantitatively not always satisfactory, and therefore we also discuss the construction of corrections to KS SCE. In particular, we investigate here a simple local correction, which, however, turns out to give rather disappointing results, suggesting that to further improve KS SCE, we need semilocal or fully nonlocal density functionals.

The paper is organized as follows. In Sec. II, we describe the KS-SCE approach, illustrating and discussing its features beyond what was reported in Ref. 49. In Sec. III, we introduce the quasi-1D systems we have addressed, and in Sec. IV we present our results, comparing the performances of KS SCE with the "exact" CI results, with the standard KS-LDA method, and discussing KS SCE with a simple local correction. Finally, in Sec. V, we draw some conclusions, as well as an outlook for future works. Hartree (effective) atomic units are used throughout the paper.

II. THEORY AND METHODOLOGY

A. KS and SCE DFT

In the formulation of Hohenberg and Kohn,[22] the ground-state density and energy of a many-electron system are obtained by minimizing the energy density functional

$$E[\rho] = F[\rho] + \int d\mathbf{r}\, v_{\text{ext}}(\mathbf{r})\, \rho(\mathbf{r}) \tag{1}$$

with respect to the density $\rho(\mathbf{r})$. In Eq. (1), $v_{\text{ext}}(\mathbf{r})$ is the external potential and $F[\rho]$ is a universal functional of the density, defined as the minimum of the internal energy (kinetic energy $\hat{T}$ plus electron-electron repulsion $\hat{V}_{ee}$) with respect to all the fermionic wave functions Ψ that yield the density $\rho(\mathbf{r})$ (Ref. 50):

$$F[\rho] = \min_{\Psi\to\rho} \langle \Psi | \hat{T} + \hat{V}_{ee} | \Psi \rangle. \tag{2}$$

In order to capture the fermionic nature of the electronic density, Kohn and Sham[23] introduced the functional $T_s[\rho]$ by minimizing the expectation value of $\hat{T}$ alone over all the fermionic wave functions yielding the given $\rho(\mathbf{r})$ (Ref. 50):

$$T_s[\rho] = \min_{\Psi\to\rho} \langle \Psi | \hat{T} | \Psi \rangle, \tag{3}$$

thus introducing a reference system of noninteracting electrons with the same density as the physical, interacting, one. The remaining part of $F[\rho]$, defining the Hartree and the exchange-correlation functionals $F[\rho] - T_s[\rho] \equiv E_{\text{Hxc}}[\rho] \equiv E_{\text{H}}[\rho] + E_{\text{xc}}[\rho]$, is then approximated. The minimization of the total energy functional $E[\rho]$ with respect to the density yields the well-known single-particle Kohn-Sham equations[23]

$$\left(-\tfrac{1}{2}\nabla^2 + v_{\text{KS}}[\rho](\mathbf{r})\right)\phi_i(\mathbf{r}) = \varepsilon_i \phi_i(\mathbf{r}), \tag{4}$$

where $v_{\text{KS}}(\mathbf{r}) \equiv v_{\text{ext}}(\mathbf{r}) + \delta E_{\text{Hxc}}[\rho]/\delta\rho(\mathbf{r}) \equiv v_{\text{ext}}[\rho](\mathbf{r}) + v_H[\rho](\mathbf{r}) + v_{\text{xc}}[\rho](\mathbf{r})$ is the one-body local Kohn-Sham potential, with $v_H[\rho](\mathbf{r})$ and $v_{\text{xc}}[\rho](\mathbf{r})$ being, respectively, the Hartree and the exchange-correlation parts. The solutions ϕ_i of Eqs. (4) are the so-called Kohn-Sham orbitals, which yield the electronic density through the relation $\rho(\mathbf{r}) = \sum_i |\phi_i(\mathbf{r})|^2$, with the sum running only over occupied orbitals. Notice that here we work with the original, spin-restricted KS scheme, in which we have the same KS potential for spin-up and -down electrons.

The HK functional of Eq. (2) and the KS functional of Eq. (3) can be seen as the particular values at $\lambda = 1$ and at $\lambda = 0$ of a more general functional $F_\lambda[\rho]$ in which the coupling-strength interaction is rescaled with a real parameter λ, i.e.,

$$F_\lambda[\rho] = \min_{\Psi\to\rho} \langle \Psi | \hat{T} + \lambda \hat{V}_{ee} | \Psi \rangle. \tag{5}$$

A well-known exact formula for the Hartree-exchange-correlation functional $E_{\text{Hxc}}[\rho]$ is[51,52]

$$E_{\text{Hxc}}[\rho] = \int_0^1 \langle \Psi_\lambda[\rho] | V_{ee} | \Psi_\lambda[\rho] \rangle\, d\lambda \equiv \int_0^1 V_{ee}^\lambda[\rho]\, d\lambda, \tag{6}$$

where $\Psi_\lambda[\rho]$ is the minimizing wave function in Eq. (5).

In the strictly-correlated-electrons DFT (SCE-DFT) formalism, one considers the strong-interaction limit of the Hohenberg-Kohn functional, $\lambda \to \infty$, which corresponds to the functional[53–56]

$$V_{ee}^{\text{SCE}}[\rho] \equiv \min_{\Psi\to\rho} \langle \Psi | \hat{V}_{ee} | \Psi \rangle, \tag{7}$$

i.e., the minimum of the electronic interaction alone over all the wave functions yielding the given density $\rho(\mathbf{r})$. This

limit has been first studied in the seminal work of Seidl and co-workers,[53–55] and later formalized and evaluated exactly in a rigorous mathematical way in Refs. 48 and 56–58. The functional $V_{ee}^{\rm SCE}[\rho]$ also defines a reference system complementary to the noninteracting one of the Kohn-Sham kinetic energy $T_s[\rho]$, namely one composed by infinitely correlated electrons, with zero kinetic energy. This implies that, analogously as in a set of confined classical repulsive charges, which arrange themselves seeking for the stable spatial configuration that minimizes their interaction energy, in the SCE reference system the position of one electron uniquely determines the position of the remaining ones, always under the constraint imposed by Eq. (7) that the density at each point is equal to that of the quantum-mechanical system with $\lambda = 1$, $\rho(\mathbf{r})$.

More precisely, the functional $V_{ee}^{\rm SCE}[\rho]$ is constructed[56] by considering that the admissible configurations of N electrons in d dimensions are restricted to a d-dimensional subspace Ω_0 of the full classical Nd-dimensional configuration space. A generic point of Ω_0 has the form

$$\mathbf{R}_{\Omega_0}(\mathbf{s}) = (\mathbf{f}_1(\mathbf{s}), \ldots, \mathbf{f}_N(\mathbf{s})), \tag{8}$$

where $\mathbf{s}$ is a d-dimensional vector that determines the position of, say, electron "1," and $\mathbf{f}_i(\mathbf{s})$ $(i = 1, \ldots, N)$, with $\mathbf{f}_1(\mathbf{s}) = \mathbf{s}$, are the so-called comotion functions, which determine the position of the ith electron as a function of $\mathbf{s}$. The comotion functions are implicit nonlocal functionals of the given density $\rho(\mathbf{r})$,[47,56,58,59] and solution of a set of differential equations that ensure the invariance of ρ under the coordinate transformation $\mathbf{s} \to \mathbf{f}_i(\mathbf{s})$, i.e.,

$$\rho(\mathbf{f}_i(\mathbf{s}))d\mathbf{f}_i(\mathbf{s}) = \rho(\mathbf{s})d\mathbf{s} \tag{9}$$

or, equivalently, that the probability of finding the electron i at $\mathbf{f}_i(\mathbf{s})$ is equal to that of finding the electron "1" at $\mathbf{s}$. At the same time, the $\mathbf{f}_i(\mathbf{s})$ must satisfy group properties that ensure the indistinguishability of the N electrons.[56,58]

The functional $V_{ee}^{\rm SCE}[\rho]$ can then be written in terms of the comotion functions $\mathbf{f}_i$ as[56,60]

$$\begin{aligned} V_{ee}^{\rm SCE}[\rho] &= \int d\mathbf{s} \frac{\rho(\mathbf{s})}{N} \sum_{i=1}^{N-1} \sum_{j=i+1}^{N} \frac{1}{|\mathbf{f}_i(\mathbf{s}) - \mathbf{f}_j(\mathbf{s})|} \\ &= \frac{1}{2} \int d\mathbf{s}\, \rho(\mathbf{s}) \sum_{i=2}^{N} \frac{1}{|\mathbf{s} - \mathbf{f}_i(\mathbf{s})|}, \end{aligned} \tag{10}$$

just as $T_s[\rho]$ is written in terms of the Kohn-Sham orbitals $\phi_i(\mathbf{r})$. The equivalence of the two expressions for $V_{ee}^{\rm SCE}[\rho]$ in Eq. (10) has been proven in Ref. 60.

Since in the SCE system the position of one electron determines all the other $N-1$ relative positions, the net repulsion felt by an electron at position $\mathbf{r}$ due to the other $N-1$ electrons becomes a function of $\mathbf{r}$ itself. For a given density $\rho_0(\mathbf{r})$, this effect can be *exactly* transformed[47,56,58] into a local one-body effective external potential $v_{\rm SCE}[\rho_0](\mathbf{r})$ that compensates the total Coulomb force on each electron when all the particles are at their respective positions $\mathbf{f}_i[\rho_0](\mathbf{r})$, i.e., such that[56]

$$\nabla v_{\rm SCE}[\rho_0](\mathbf{r}) = \sum_{i=2}^{N} \frac{\mathbf{r} - \mathbf{f}_i[\rho_0](\mathbf{r})}{|\mathbf{r} - \mathbf{f}_i[\rho_0](\mathbf{r})|^3}. \tag{11}$$

In terms of the classical-charge analog, $v_{\rm SCE}[\rho_0](\mathbf{r})$ can thus be seen as an external potential for which the total classical potential energy

$$E_{\rm pot}(\mathbf{r}_1, \ldots \mathbf{r}_N) \equiv \sum_{i=1}^{N-1} \sum_{j=i+1}^{N} \frac{1}{|\mathbf{r}_i - \mathbf{r}_j|} + \sum_{i=1}^{N} v_{\rm SCE}[\rho_0](\mathbf{r}_i) \tag{12}$$

is minimum when the electronic positions reside on the subset $\mathbf{R}_{\Omega_0}$, i.e., when $\mathbf{r}_i = \mathbf{f}_i[\rho_0](\mathbf{r})$ or, equivalently, when the associated density at each point is equal to $\rho_0(\mathbf{r})$. For an arbitrary density $\rho(\mathbf{r})$, the potential-energy density functional defined as

$$E_{\rm pot}^{\rm SCE}[\rho] \equiv V_{ee}^{\rm SCE}[\rho] + \int v_{\rm SCE}[\rho_0](\mathbf{r})\rho(\mathbf{r})d\mathbf{r} \tag{13}$$

will then satisfy the stationarity condition $\delta E_{\rm pot}^{\rm SCE}[\rho]/\delta\rho(\mathbf{r})|_{\rho=\rho_0} = 0$, i.e., we will have that

$$\left.\frac{\delta V_{ee}^{\rm SCE}[\rho]}{\delta\rho(\mathbf{r})}\right|_{\rho=\rho_0} = -v_{\rm SCE}[\rho_0](\mathbf{r}). \tag{14}$$

Notice that Eq. (14) involves the functional derivative of a highly nonlocal implicit functional of the density, defined by Eqs. (9) and (10). This, however, turns out to reduce to a local one-body potential that can be easily calculated from the integration of Eq. (11) once the comotion functions are obtained via Eq. (9). This shortcut to compute the functional derivative of $V_{ee}^{\rm SCE}[\rho]$ is extremely powerful for including strong correlation in the KS formalism.[49]

B. Zeroth-order KS-SCE approach

Equations (11) and (14) show how the effects of strong correlation, captured by the limit $\lambda \to \infty$ of $F_\lambda[\rho]$ and rigorously represented by the highly nonlocal functional $V_{ee}^{\rm SCE}[\rho]$, are *exactly* transferred into the one-body potential $v_{\rm SCE}[\rho]$. The KS-SCE approach to zeroth order consists in using this property to approximate the Hartree-exchange-correlation term of the Kohn-Sham potential as

$$\frac{\delta E_{\rm Hxc}[\rho]}{\delta\rho(\mathbf{r})} \approx \tilde{v}_{\rm SCE}[\rho](\mathbf{r}), \quad \tilde{v}_{\rm SCE}[\rho](\mathbf{r}) \equiv -v_{\rm SCE}[\rho](\mathbf{r}). \tag{15}$$

Notice that we have defined $\tilde{v}_{\rm SCE}[\rho](\mathbf{r}) = -v_{\rm SCE}[\rho](\mathbf{r})$, as here we seek an effective potential for KS theory, which corresponds to the net electron-electron repulsion acting on an electron at position $\mathbf{r}$, while the effective potential for the SCE system of Eq. (11) *compensates* the net electron-electron repulsion.

More rigorously, by considering the $\lambda \to \infty$ expansion of the integrand of Eq. (6), one obtains[53–56,59]

$$V_{ee}^{\lambda\to\infty}[\rho] = V_{ee}^{\rm SCE}[\rho] + \frac{V_{ee}^{\rm ZPE}[\rho]}{\sqrt{\lambda}} + O(\lambda^{-p}), \tag{16}$$

where the acronym "ZPE" stands for "zero-point energy," and $p \geqslant \frac{5}{4}$ (see Ref. 59 for further details). By inserting the expansion of Eq. (16) into Eq. (6), one obtains an approximation for $E_{\rm Hxc}[\rho]$:

$$E_{\rm Hxc}[\rho] \approx V_{ee}^{\rm SCE}[\rho] + 2\,V_{ee}^{\rm ZPE}[\rho] + \cdots. \tag{17}$$

We consider here only the first term, corresponding to a zeroth-order expansion around $\lambda = \infty$, i.e., $E_{\rm Hxc}[\rho] \approx V_{ee}^{\rm SCE}[\rho]$, which yields Eq. (15) for the corresponding functional derivatives.

Taking into account the definition of the functional $V_{ee}^{\rm SCE}[\rho]$ [Eq. (7)], the zeroth-order KS SCE is equivalent to approximate the minimization over Ψ in the HK functional of Eq. (2) as

$$\min_{\Psi\to\rho}\langle\Psi|\hat{T}+\hat{V}_{ee}|\Psi\rangle \approx \min_{\Psi\to\rho}\langle\Psi|\hat{T}|\Psi\rangle + \min_{\Psi\to\rho}\langle\Psi|\hat{V}_{ee}|\Psi\rangle = T_s[\rho] + V_{ee}^{\rm SCE}[\rho]. \tag{18}$$

The KS-SCE approach thus treats both the kinetic energy and the electron-electron repulsion on the same footing, combining the advantages of both KS and SCE DFT and therefore allowing one to address both the weakly and the strongly interacting regimes, as well as the crossover between them.[49] Indeed, from the scaling properties[61] of the functionals $F[\rho]$, $T_s[\rho]$, and $V_{ee}^{\rm SCE}[\rho]$, it derives that the approximation of Eq. (18) becomes accurate both in the weak- and in the strong-interaction limits, while probably less precise in-between. To use the scaling relations,[61] one defines, for electrons in D dimensions, a scaled density

$$\rho_\gamma(\mathbf{r}) \equiv \gamma^D \rho(\gamma\,\mathbf{r}), \qquad \gamma > 0.$$

We then have[48,61]

$$T_s[\rho_\gamma] = \gamma^2\, T_s[\rho], \tag{19}$$

$$V_{ee}^{\rm SCE}[\rho_\gamma] = \gamma\, V_{ee}^{\rm SCE}[\rho], \tag{20}$$

$$F[\rho_\gamma] = \gamma^2\, F_{1/\gamma}[\rho], \tag{21}$$

where $F_{1/\gamma}[\rho]$ means[61] that the Coulomb coupling constant λ in $F_\lambda[\rho]$ of Eq. (5) has been set equal to $1/\gamma$. We then see that both sides of Eq. (18) tend to $T_s[\rho_\gamma]$ when $\gamma\to\infty$ (high-density or weak-interaction limit) and to $V_{ee}^{\rm SCE}[\rho_\gamma]$ when $\gamma\to 0$ (low-density or strong-interaction limit).

Standard KS DFT emphasizes the noninteracting shell structure, properly described through the functional $T_s[\rho]$, but it misses the features of strong correlation. SCE DFT, on the contrary, is biased towards localized "Wigner-type" structures in the density, accurately described by $V_{ee}^{\rm SCE}[\rho]$, missing the fermionic shell structure. Many interesting systems lie in-between the weakly and the strongly interacting limits, and their complex behavior arises precisely from the competition between the fermionic structure embodied in the kinetic energy and correlation effects due to the electron-electron repulsion. By implementing the exact $\tilde{v}_{\rm SCE}[\rho](\mathbf{r})$ potential in the Kohn-Sham scheme, we thus let these two factors compete in a self-consistent procedure.[49]

One should also notice that while the KS-SCE approach does not use explicitly the Hartree functional, the correct electrostatics is still captured since $V_{ee}^{\rm SCE}[\rho]$ is the classical electrostatic minimum in the given density ρ. Moreover, the potential $\tilde{v}_{\rm SCE}[\rho](\mathbf{r})$ stems from a wave function (the SCE one[56,59]) and is therefore completely self-interaction free.

Finally, another neat property of the zeroth-order KS-SCE approach is that it always yields a lower bound to the exact ground-state energy $E_0 = E[\rho_0]$, where ρ_0 is the exact ground-state density. In fact, for any given ρ, the right-hand side of Eq. (18) is always less or equal than the left-hand side, as the minimum of a sum is always larger than the sum of the minima. As a consequence, for $\rho = \rho_0$ we have the inequality

$$E[\rho_0] = F[\rho_0] + \int \rho_0\, v_{\rm ext} \geqslant T_s[\rho_0] + V_{ee}^{\rm SCE}[\rho_0] + \int \rho_0\, v_{\rm ext}, \tag{22}$$

which becomes even stronger when ones minimizes the functional on the right-hand-side with respect to the density within the self-consistent zeroth-order KS-SCE procedure. It should be noted that this property implies an important difference with respect to the variational wave-function methods (such as HF, CI, QMC, and DMRG), which, instead, provide an upper bound to the exact ground-state energy.

C. Local correction to zeroth-order KS SCE

As preliminarily found in Ref. 49 and further shown in Sec. IV, the zeroth-order KS SCE yields results that are qualitatively correct in the strong-correlation regime (representing a significative conceptual advance for KS DFT), but still with quantitative errors, which become smaller and smaller as correlation increases. An important issue is thus to add corrections to Eq. (18). One can, more generally, decompose $F[\rho]$ as

$$F[\rho] = T_s[\rho] + V_{ee}^{\rm SCE}[\rho] + T_c[\rho] + V_{ee}^{d}[\rho], \tag{23}$$

where $T_c[\rho]$ (kinetic correlation energy) is

$$T_c[\rho] = \langle\Psi[\rho]|\hat{T}|\Psi[\rho]\rangle - T_s[\rho], \tag{24}$$

i.e., the difference between the true kinetic energy and the Kohn-Sham one, and $V_{ee}^{d}[\rho]$ (electron-electron decorrelation energy) is

$$V_{ee}^{d}[\rho] = \langle\Psi[\rho]|\hat{V}_{ee}|\Psi[\rho]\rangle - V_{ee}^{\rm SCE}[\rho], \tag{25}$$

i.e., the difference between the true expectation of $\hat{V}_{ee}$ and the SCE value. A "first-order" approximation for $T_c[\rho] + V_{ee}^{d}[\rho]$ can be obtained from Eq. (17),

$$T_c[\rho] + V_{ee}^{d}[\rho] \approx 2\, V_{ee}^{\rm ZPE}[\rho], \tag{26}$$

and can be, in principle, included exactly using the formalism developed in Ref. 59, but other approximations, e.g., in the spirit of Ref. 62, can also be constructed.

Here, we consider an even simpler approximation: $T_c[\rho] + V_{ee}^{d}[\rho] \approx E_{\rm LC}[\rho]$, where $E_{\rm LC}[\rho]$ is a local term that includes, at each point of space $\mathbf{r}$, the corresponding correction for a uniform electron gas with the same local density $\rho(\mathbf{r})$, i.e.,

$$E_{\rm LC}[\rho] = \int \rho(\mathbf{r})\left\{t_c[\rho(\mathbf{r})] + v_{ee}^{d}[\rho(\mathbf{r})]\right\} d\mathbf{r}. \tag{27}$$

In Eq. (27), $t_c(\rho)$ and $v_{ee}^{d}(\rho)$ are the kinetic correlation energy and the electron-electron decorrelation energy per particle of an electron gas with uniform density ρ, corresponding to

$$t_c(\rho) + v_{ee}^{d}(\rho) = \epsilon_{xc}(\rho) - \epsilon_{\rm SCE}(\rho), \tag{28}$$

where $\epsilon_{xc}(\rho)$ is the usual electron-gas exchange-correlation energy and $\epsilon_{\rm SCE}(\rho)$ is the indirect part (expectation of $\hat{V}_{ee}$ minus the Hartree energy) of the SCE interaction energy per

electron of the uniform electron gas with density ρ. This correction makes the approximate internal energy functional

$$F[\rho] = T_s[\rho] + V_{ee}^{\mathrm{SCE}}[\rho] + E_{\mathrm{LC}}[\rho] \tag{29}$$

become exact in the limit of uniform density, similarly to what the LDA functional does in standard KS DFT.

III. MODEL AND DETAILS OF THE CALCULATIONS

We consider N electrons in the quasi-one-dimensional (Q1D) model quantum wire of Refs. 28 and 63:

$$\hat{H} = -\frac{1}{2}\sum_{i=1}^{N}\frac{\partial^2}{\partial x_i^2} + \sum_{i=1}^{N-1}\sum_{j=i+1}^{N} w_b(|x_i - x_j|) + \sum_{i=1}^{N} v_{\mathrm{ext}}(x_i), \tag{30}$$

in which the effective electron-electron interaction is obtained by integrating the Coulomb repulsion on the lateral degrees of freedom,[63,64] and is given by

$$w_b(x) = \frac{\sqrt{\pi}}{2b}\exp\left(\frac{x^2}{4b^2}\right)\mathrm{erfc}\left(\frac{x}{2b}\right). \tag{31}$$

The parameter b fixes the thickness of the wire, set to $b = 0.1$ throughout this study, and $\mathrm{erfc}(x)$ is the complementary error function. The interaction $w_b(x)$ has a long-range Coulombic tail $w_b(x \to \infty) = 1/x$, and is finite at the origin, where it has a cusp. As in Ref. 28, we consider an external harmonic confinement $v_{\mathrm{ext}}(x) = \frac{1}{2}\omega^2 x^2$ in the direction of motion of the electrons. The wire can be characterized by an effective confinement-length parameter L such that

$$\omega = \frac{4}{L^2}, \quad v_{\mathrm{ext}}(x) = \frac{1}{2}\omega^2 x^2.$$

A. Zeroth-order KS SCE

The comotion functions $f_i(x)$ can be constructed by integrating Eqs. (9) for a given density $\rho(x)$,[53,57,58] choosing boundary conditions that make the density between two adjacent strictly correlated positions always integrate to unity (total suppression of fluctuations),[53]

$$\int_{f_i(x)}^{f_{i+1}(x)} \rho(x')\,dx' = 1, \tag{32}$$

and ensuring that the $f_i(x)$ satisfy the required group properties.[53,56,58] This yields

$$f_i(x) = \begin{cases} N_e^{-1}[N_e(x) + i - 1], & x \leqslant a_{N+1-i} \\ N_e^{-1}[N_e(x) + i - 1 - N], & x > a_{N+1-i} \end{cases} \tag{33}$$

where the function $N_e(x)$ is defined as

$$N_e(x) = \int_{-\infty}^{x} \rho(x')\,dx', \tag{34}$$

and $a_k = N_e^{-1}(k)$. Equation (11) becomes in this case

$$\tilde{v}'_{\mathrm{SCE}}[\rho](x) = \sum_{i=2}^{N} w_b'[|x - f_i(x)|]\mathrm{sgn}[x - f_i(x)]. \tag{35}$$

We then solve self-consistently the Kohn-Sham equations (4) with the KS potential $v_{\mathrm{KS}}(x) = v_{\mathrm{ext}}(x) + \tilde{v}_{\mathrm{SCE}}[\rho](x)$, where $\tilde{v}_{\mathrm{SCE}}[\rho](x)$ is obtained by integrating Eq. (35) with the boundary condition $\tilde{v}_{\mathrm{SCE}}[\rho](|x| \to \infty) = 0$. As said, we work in the spin-restricted KS framework, in which each spatial orbital is doubly occupied.

B. Configuration interaction method (CI)

In the configuration interaction calculations, the full many-body wave function is expanded as a linear combination of Slater determinants, constructed with the noninteracting harmonic oscillator orbitals. A matrix representation of the Hamiltonian in this basis is then numerically diagonalized to find the eigenstates of the system. The number of possible ways to place N particles in a given set of orbitals increases rapidly as a function of N, such that only small particle numbers are tractable. Also, the stronger the interaction, the more basis orbitals are generally required to obtain a good approximation. For the present physical system, about 20–40 orbitals were needed to get converged solutions, which resulted in Hilbert space dimensions in the range 10^5–10^6. For a more detailed description of the method, see, e.g., Refs. 65 and 66.

C. KS LDA

We have performed Kohn-Sham LDA calculations using the exchange-correlation energy per particle $\epsilon_{\mathrm{xc}} = \epsilon_x + \epsilon_c$ for a 1D homogeneous electron gas with the renormalized Coulomb interaction $w_b(x)$, as detailed in Ref. 28. The exchange term ϵ_x is given by

$$\epsilon_x(r_s) = \frac{1}{2}\int_{-\infty}^{+\infty}\frac{dq}{2\pi} v_b(q)\,[S_0(q) - 1]\,, \tag{36}$$

where $v_b(q)$ is the Fourier transform of the interaction potential, $S_0(q)$ is the noninteracting static structure factor, and $r_s \equiv \frac{1}{2\rho}$.[67] To increase the numerical stability, we have interpolated between the Taylor expansions of $\epsilon_x(r_s)$ at small and large r_s up to order 14. For the correlation term, we have used the results of Casula *et al.*,[68] who have parametrized their QMC data as

$$\epsilon_c(r_s) = -\frac{r_s}{A + Br_s^{\gamma_1} + Cr_s^2}\ln\left(1 + Dr_s + Er_s^{\gamma_2}\right), \tag{37}$$

where the different parameters are given in Table IV of Ref. 68 for several values of b.

D. KS SCE with local correction

We have obtained the indirect SCE energy per electron $\epsilon_{\mathrm{SCE}}(\rho)$ needed in Eq. (28) by first computing the indirect $\epsilon_{\mathrm{SCE}}^{\mathrm{drop}}(\rho, N)$ for a 1D droplet with N electrons, uniform density ρ, and radius $R = \frac{N}{2\rho}$, as described in Ref. 57. We have then evaluated the limit $N \to \infty$ at fixed density ρ to obtain the bulk value. The details of this calculation are reported in the Appendix.

In Fig. 1, we show our numerical results for $b = 0.1$ compared to the parametrized[68] QMC results for the exchange-correlation energy $\epsilon_{\mathrm{xc}}(r_s)$ of Eqs. (36) and (37). We see that, as it should be, $\epsilon_{\mathrm{SCE}}(r_s) \leqslant \epsilon_{xc}(r_s)$ everywhere. For large r_s, we find that the SCE data are very close to the QMC parametrization, with differences of the order of $\sim 0.1\%$. Notice also that at $r_s = 0$ we have $\epsilon_{\mathrm{SCE}}(0) = \epsilon_{xc}(0) = \epsilon_x(0) =$

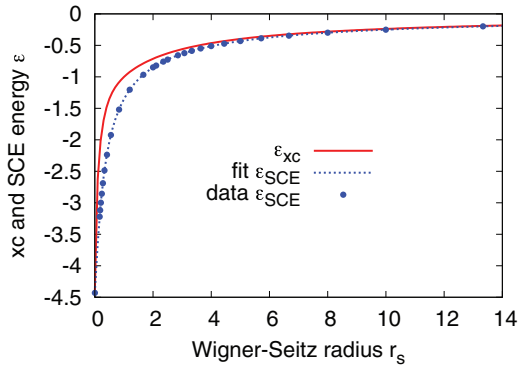

FIG. 1. (Color online) The indirect SCE energy $\epsilon_{\rm SCE}(r_s)$ for the 1D gas [interaction of Eq. (31) and $b = 0.1$] is compared to the parametrized QMC data (Ref. 68) for the exchange-correlation energy $\epsilon_{\rm xc}(r_s)$. For the SCE energy, we show both our numerical results and the fitting function of Eqs. (38) and (39).

$-\frac{\sqrt{\pi}}{4b}$. This is due to the fact that in the $r_s \to 0$ limit at fixed b, the first-order perturbation to the noninteracting gas is just a constant, so that every normalized wave function yields the same result for the leading term. We have parametrized our data for $\epsilon_{\rm SCE}(r_s)$ as

$$\epsilon_{\rm SCE}(\rho) = \rho\, q(2\,b\,\rho), \tag{38}$$

with

$$q(x) = A_1 \ln\left(\frac{a_1 x + a_2 x^2}{1 + a_3 x + a_2 x^2}\right), \tag{39}$$

and $A_1 = 0.992\,453\,4$, $a_2 = 1.551\,767\,43$, $a_3 = 2.025\,166\,778$, $a_1 = a_3 - \frac{a_2\sqrt{\pi}}{2A_1}$. This fit is valid for all values of b since the scaling of Eq. (38) is exact for the SCE energy. The fitting function is also shown in Fig. 1 for the case $b = 0.1$.

IV. RESULTS

Figure 2 shows the electron densities for $N = 4$ and different effective confinement lengths $L = 2\omega^{-1/2}$ obtained with the KS-SCE, the CI, and the KS-LDA approaches. One can see that the three methods show qualitative agreement in the weakly correlated regime, represented here in Fig. 2(a) by the case $L = 1$. The densities have $N/2$ peaks, given by the Friedel-type oscillations with wave number $2k_F^{\rm eff}$, where $k_F^{\rm eff} = \pi\tilde{\rho}/2$ is the effective Fermi wave number, determined by the average density in the bulk of the trap $\tilde{\rho}$.

As the confinement length of the wire increases, the interactions start to become dominant and, whereas the KS-SCE and the CI results are still in qualitative agreement, the LDA clearly provides a physically wrong description of the system. Indeed, one can see from Fig. 2(b) that whereas the densities obtained from the KS-SCE and the CI methods develop a four-peak structure, corresponding to charge localization and indicating that the system enters the crossover between the weakly and the strongly correlated regimes (the $2k_F \to 4k_F$ crossover), the KS LDA yields a flat density. This is a typical error of local and semilocal density functionals that shows up also in bond breaking (yielding wrong molecular dissociation curves) and in systems close to the Mott insulating regime. In such cases,

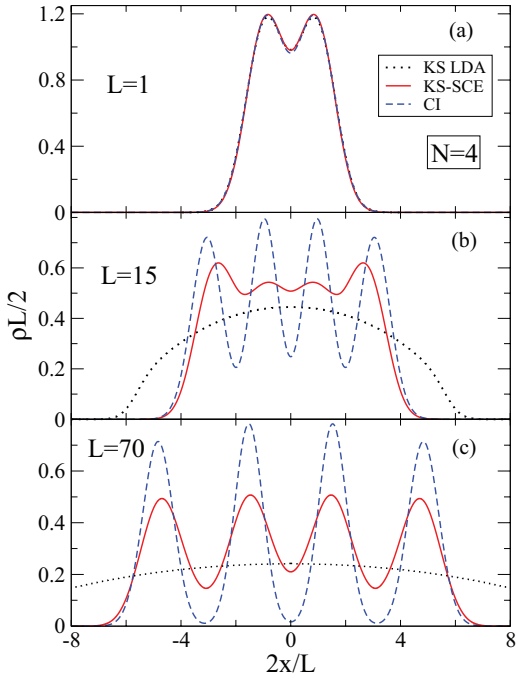

FIG. 2. (Color online) Electron densities for $N = 4$ and $L = 1$, 15, and 70, obtained with the KS-SCE, CI, and KS LDA approaches. The results are given in units of the effective confinement length $L = 2\omega^{-1/2}$.

better total energies are obtained by using spin-dependent functionals and allowing symmetry breaking. This, however, does not yield a satisfactory physical description of such systems, missing many key features and giving a wrong characterization of several properties (see, e.g., Refs. 21, 24, and 27).

When the system becomes even more strongly correlated, here represented by $L = 70$, the KS SCE gets closer to the CI result, with densities that clearly present N peaks, corresponding to charge localization. The KS-LDA density is now very delocalized and almost flat in the scale of Fig. 2. In order to obtain charge localization within the restricted KS scheme, the self-consistent KS potential must build "bumps" (or barriers) between the electrons. These barriers are a very nonlocal effect and are known to be a key property of the exact Kohn-Sham potential, as discussed in Refs. 30 and 39.

In Fig. 3, we show that the self-consistent KS-SCE scheme builds, indeed, the above-mentioned barriers in the corresponding Kohn-Sham potentials, which we plot together with the corresponding densities for $N = 4$ and 5 for $L = 70$. One can see that each of the N peaks in the density corresponds to a minimum in the KS potential, which is separated from the neighboring ones by barriers or "bumps," at whose maxima the KS potential has a discontinuous (but finite[58]) first derivative. The number of such barriers is thus equal to $N - 1$, and they become more pronounced with increasing correlation, enhancing the corresponding charge localization. Notice that the discontinuous first derivative of the KS-SCE potential at the barrier maxima is a feature due to the classical nature of the SCE potential, and it is not expected to appear in the exact KS potential (indeed, it does not appear in any of the available calculations of the "exact" KS potential obtained by inversion).

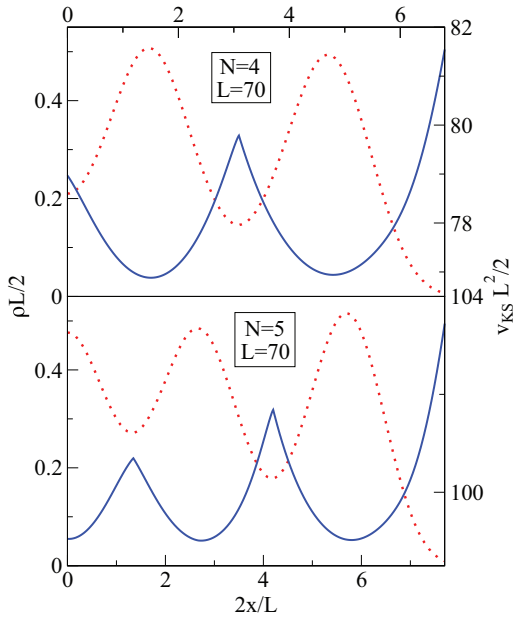

FIG. 3. (Color online) Self-consistent Kohn-Sham potentials obtained with the KS-SCE method for $N = 4$ and 5, with effective confinement length $L = 70$ (blue solid lines). The corresponding densities are also shown (red dotted lines). Notice that for the sake of clarity, only the results for $x > 0$ are shown. The results are given in units of the effective confinement length $L = 2\omega^{-1/2}$.

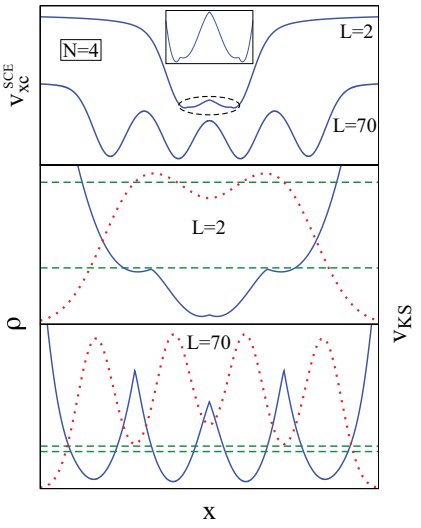

FIG. 4. (Color online) Top panel: self-consistent KS-SCE exchange-correlation (xc) potential for $N = 4$ at weak correlation ($L = 2$) and strong correlation ($L = 70$). In the inset, the oscillating part of the xc potential at $L = 2$ is zoomed in. Middle panel: total self-consistent KS-SCE potential (blue, solid line), the corresponding density (red dotted line), and the two occupied KS eigenvalues (green dashed horizontal lines) for the weakly correlated $L = 2$ wire. In this case, we see that in the KS system there are no classically forbidden regions inside the trap. Bottom panel: the same as in the middle panel for the strongly correlated $L = 70$ wire. In this case, we clearly see the classically forbidden regions inside the trap created by the barriers in the KS-SCE potential. The results are given in arbitrary units.

It is also interesting to make a connection between our results and the recent work on the KS exchange-correlation potential for the 1D Hubbard chains.[45,69,70] In particular, Vieira[45] has shown that the exact exchange-correlation potential for a 1D Hubbard chain with hopping parameter t and onsite interaction U, obtained by inversion from the exact many-body solution, always oscillates with frequency $4k_F$, while the density oscillations undergo a $2k_F \rightarrow 4k_F$ crossover with increasing U/t. The crossover in the density is thus due to the increase in the amplitude of the oscillations of the xc potential. In Fig. 4, we show the KS-SCE exchange-correlation potentials for $N = 4$ electrons in the weakly ($L = 2$) and strongly ($L = 70$) correlated regimes. We see that the KS-SCE self-consistent results are in qualitative agreement with the findings of Vieira:[45] the oscillations in the xc potential have essentially a frequency $4k_F$ also in the weakly correlated case, with amplitude that increases with increasing L [due to the scaling of Eqs. (19)–(21), the parameter L plays here a role similar to U/t for the Hubbard chain]. In the two lower panels of the same figure, we also further clarify the $2k_F \rightarrow 4k_F$ crossover in the KS framework: we see that the $4k_F$ regime in the density oscillations occurs when the barriers in the total KS potential (due to the large oscillations of the xc potential) are large enough to create classically forbidden regions inside the trap for the occupied KS orbitals.

In Table I, we report the total energies obtained with the three approaches KS SCE, CI, and KS LDA, for different values of the parameters L and N. It can be seen that in the weakly correlated regime, represented here by $L = 1$ and 2, the error made by the KS-SCE approach is larger than the one corresponding to the KS LDA. The results also clearly show that, as previously discussed, KS SCE is always a lower bound to the total energy. As the system becomes more correlated, the results obtained with the KS-SCE and the CI approaches become closer to each other, whereas the value given by the KS LDA is less accurate, as one could have inferred from the corresponding densities shown in panels Figs. 2(b) and 2(c).

In the exact Kohn-Sham theory, the highest occupied KS eigenvalue is equal to minus the exact chemical potential from the electron-deficient side,[71,72] i.e., $\mu^- = E_{N-1} - E_N$. In Table II, we compare the highest occupied KS eigenvalue obtained with the KS-SCE and the KS-LDA approaches with the values of $E_N - E_{N-1}$ calculated from the total energies given by the CI method, corresponding to the same values of N and L given in Table I. One can see that in this case

TABLE I. Comparison of the total energies obtained with the KS-SCE, CI, and KS-LDA approaches for different values of the particle number N and effective-confinement length $L = 2\omega^{-1/2}$.

N	L	KS SCE	CI	KS LDA
2	2	1.81	2.49	2.59
2	15	0.0942	0.106	0.130
2	70	0.0112	0.0115	0.0182
4	1	25.08	28.42	28.57
4	2	8.46	10.60	10.68
4	15	0.491	0.541	0.580
4	70	0.0602	0.0629	0.0771
5	15	0.787	0.871	0.915
5	70	0.099	0.102	0.121

TABLE II. For the same systems of Table I, we compare the highest occupied KS eigenvalues obtained from KS SCE and KS LDA with the full CI values of $E_N - E_{N-1}$.

N	L	KS SCE	CI	KS LDA
2	2	1.65	1.99	2.56
2	15	0.104	0.097	0.263
2	70	0.0126	0.0111	0.040 87
4	1	11.26	11.86	12.56
4	2	4.08	4.65	5.02
4	15	0.248	0.256	0.453
4	70	0.0318	0.0304	0.069 09
5	15	0.325	0.330	0.539
5	70	0.0408	0.0391	0.081 72

the KS SCE gives good results also in the weakly correlated regime. In the strongly correlated limit, the KS-SCE and the CI results show an agreement similar to that observed in the corresponding total energies. KS LDA, as usual, yields too high eigenvalues, due to the too fast decay of the exchange-correlation potential for $|x| \to \infty$.

As mentioned earlier, the numerical cost of the CI method increases exponentially with the number of particles, and this limitation becomes stronger as the correlations become dominant. In the calculations reported above, for the five-electron case with $L = 70$, we diagonalized a matrix where the eigenvectors had a dimension of about 3.5×10^5. While it is technically possible to treat larger matrices, the rapid growth of the basis size still efficiently limits the number of particles one can handle. (For $N = 6$ electrons, using the same basis orbitals, the corresponding dimension is roughly 2.6×10^6.) The KS-SCE method, on the contrary, has a numerical cost (in 1D) comparable to the one of KS LDA, therefore allowing us to study strongly correlated systems with much larger particle numbers. In Fig. 5, we show the electron densities and corresponding KS potentials obtained with the KS-SCE

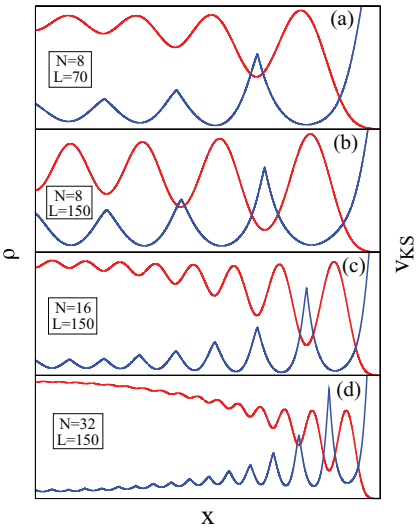

FIG. 5. (Color online) Electron density and corresponding KS-SCE potential for different particle numbers N and effective confinement lengths L. As in Fig. 3, only the results for $x > 0$ are shown. The results are given in arbitrary units.

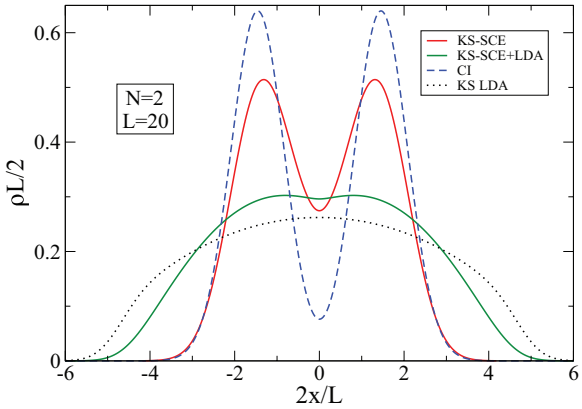

FIG. 6. (Color online) Electron density for the case $N = 2$ and $L = 20$. The "exact" CI result is compared with the KS LDA, the KS SCE, and the KS SCE with local correction of Secs. II C and III D (KS SCE + LDA) results. The results are given in units of the effective confinement length $L = 2\omega^{-1/2}$.

method for $N = 8$, 16, and 32, for different values of L: in Figs. 5(a) and 5(b) we see how, at fixed number of particles $N = 8$, the bumps in the KS potential and the amplitude of the density oscillations become larger with increasing L. For fixed effective confinement length $L = 150$, we see from Figs. 5(b)–5(d) how increasing the particle number N leads to less pronounced features of strong correlation, according to the scaling of Eqs. (19)–(21). These calculations took few minutes on a desktop computer.

Finally, we have tested the local correction to the zeroth-order KS SCE discussed in Secs. II C and III D: as we see in the case $N = 2$ and $L = 20$ reported in Fig. 6, the results for the self-consistent densities are very disappointing, laying in-between the KS-SCE and the standard KS-LDA values. This is due to the fact that, similarly to the standard KS-LDA case, this simple local correction can not capture the physics of the intermediate- and strong-correlation regimes, so that its inclusion worsens the results of KS SCE. In future work, we will explore semilocal and fully nonlocal corrections to KS SCE.

V. CONCLUSIONS AND PERSPECTIVES

We have used the exact strong-interaction limit of the Hohenberg-Kohn functional to approximate the exchange-correlation energy and potential of Kohn-Sham DFT. By means of this so-called KS-SCE approach, we have addressed quasi-one-dimensional quantum wires in the weak, intermediate, and strong regimes of correlations, comparing the results with those obtained by using the configuration interaction method and the KS local density approximation. In the weakly correlated regime, the three approaches give qualitatively similar results, with electronic densities showing $N/2$ peaks, associated with the double occupancy of the single-particle levels that dominate the system. In this regime, KS LDA performs overall better than KS SCE. As correlations become dominant, the KS-SCE and the CI densities start to develop additional maxima, corresponding to charge-density localization, whereas the KS LDA provides a qualitatively wrong description of the system, yielding a very flat, delocalized, density. We have also investigated a simple local correction to

KS SCE, which, however, gives very disappointing results. In future works, we will thus explore semilocal and fully nonlocal corrections to KS SCE.

The Kohn-Sham potential of the KS-SCE approach shows "bumps" that are responsible for the charge localization and are a well-known feature of the exact Kohn-Sham potential of strongly correlated systems. Moreover, the associated KS-SCE exchange-correlation potential shows the right asymptotic behavior since it is self-interaction free as it is constructed from a wave function (the SCE one[49,56,59]). This way, KS SCE is able to also give rather accurate chemical potentials. Notice that, as shown by studies of one-dimensional Hubbard chains, the $2k_F \to 4k_F$ crossover in the density is a very challenging task for KS DFT for nonmagnetic systems.[45,69] The fact that KS SCE is able to capture this crossover is thus a very remarkable and promising feature.

Crucial for future applications is calculating $V_{ee}^{\rm SCE}[\rho]$ and $\tilde{v}_{\rm SCE}[\rho](\mathbf{r})$ also for general two- and three-dimensional systems. An enticing route towards this goal involves the mass-transportation-theory reformulation of the SCE functional,[58] in which $V_{ee}^{\rm SCE}[\rho]$ is given by the maximum of the Kantorovich dual problem

$$\max_u \left\{ \int u(\mathbf{r})\rho(\mathbf{r})d\mathbf{r} \;:\; \sum_{i=1}^{N} u(\mathbf{r}_i) \leqslant \sum_{i=1}^{N-1}\sum_{j>i}^{N} \frac{1}{|\mathbf{r}_i - \mathbf{r}_j|} \right\},$$

where $u(\mathbf{r}) = \tilde{v}_{\rm SCE}[\rho](\mathbf{r}) + C$, and C is a constant.[58] This is a maximization under linear constraints that yields in one shot the functional and its functional derivative. Although the number of linear constraints is infinite, this formulation may lead to approximate but accurate approaches to the construction of $V_{ee}^{\rm SCE}[\rho]$ and $\tilde{v}_{\rm SCE}[\rho](\mathbf{r})$, as very recently shown by Mendl and Lin.[73]

ACKNOWLEDGMENTS

We thank M. Seidl for inspiring discussions. This work was financially supported by the Netherlands Organization for Scientific Research (NWO) through a Vidi grant and by the Swedish Research Council and the Nanometer Structure Consortium at Lund University (nmC@LU).

APPENDIX: SCE FOR THE UNIFORM Q1D ELECTRON GAS

Following Ref. 57, we have computed the SCE indirect Coulomb interaction energy per electron $\epsilon_{\rm SCE}^{\rm drop}(\rho,N)$ of a 1D droplet of uniform density ρ and radius $R = \frac{N}{2\rho}$, where N is the number of electrons,

$$\epsilon_{\rm SCE}^{\rm drop}(\rho,N) = \frac{2}{N}\,\rho\,\tilde{v}_{ee}^{\rm SCE}(2\,\rho\,b,N) - \frac{\rho}{\pi}u_1\left(\frac{2\,b\,\rho}{N}\right), \qquad \text{(A1)}$$

where

$$\tilde{v}_{ee}^{\rm SCE}(x,N) = \frac{\pi}{2x}\sum_{i=1}^{N}(N-i)e^{i^2/x^2}\,\mathrm{erfc}\left(\frac{i}{x}\right) \qquad \text{(A2)}$$

is the rescaled SCE energy of the droplet[57] and the second term in the right-hand side of Eq. (A1) is its Hartree energy, with

$$u_1(x) = \int_0^\infty \left(\frac{\sin k}{k}\right)^2 e^{k^2x^2}E_1(k^2x^2)\,dk \qquad \text{(A3)}$$

and

$$E_1(x) = \int_1^\infty \frac{e^{-tx}}{t}dt.$$

Since the function $u_1(x)$ is numerically unstable, we have interpolated between its small-x expansion through orders $O(x^5)$,

$$u_1^<(x) = \frac{\pi x^4}{16} - \frac{\pi x^2}{4} + \frac{1}{2}\pi^{3/2}x - \pi\log(x) - \frac{1}{2}\pi\psi^{(0)}\left(\frac{3}{2}\right),$$

with $\psi^{(0)}(\frac{3}{2}) \approx 0.036\,489\,974$, and its large-$x$ expansion through orders $O(x^{-16})$:

$$\begin{aligned} u_1^>(x) = {} & \frac{\pi^{3/2}}{1209600x^{15}} - \frac{64\pi}{14189175x^{14}} + \frac{\pi^{3/2}}{131040x^{13}} \\ & - \frac{16\pi}{405405x^{12}} + \frac{\pi^{3/2}}{15840x^{11}} - \frac{16\pi}{51975x^{10}} + \frac{\pi^{3/2}}{2160x^9} \\ & - \frac{2\pi}{945x^8} + \frac{\pi^{3/2}}{336x^7} - \frac{4\pi}{315x^6} + \frac{\pi^{3/2}}{60x^5} - \frac{\pi}{15x^4} \\ & + \frac{\pi^{3/2}}{12x^3} - \frac{\pi}{3x^2} + \frac{\pi^{3/2}}{2x}, \end{aligned}$$

switching between them at $x = 0.584\,756$.

We have then evaluated numerically the limit $N \to \infty$ of Eq. (A1) at fixed ρ. We have found that the convergence is reasonably fast: for example, taking $N = 10^5$ yields results with a relative accuracy of 10^{-6}. Our numerical results have been fitted with the function $q(x)$ of Eqs. (38) and (39).

[1] E. P. Wigner, Phys. Rev. **46**, 1002 (1934).
[2] C. E. Creffield, W. Hausler, J. H. Jefferson, and S. Sarkar, Phys. Rev. B **59**, 10719 (1999).
[3] R. Egger, W. Hausler, C. H. Mak, and H. Grabert, Phys. Rev. Lett. **82**, 3320 (1999).
[4] C. Yannouleas and U. Landman, Phys. Rev. Lett. **82**, 5325 (1999).
[5] S. M. Reimann, M. Koskinen, and M. Manninen, Phys. Rev. B **62**, 8108 (2000).
[6] A. V. Filinov, M. Bonitz, and Y. E. Lozovik, Phys. Rev. Lett. **86**, 3851 (2001).
[7] A. Ghosal, A. D. Guclu, C. J. Umrigar, D. Ullmo, and H. U. Baranger, Phys. Rev. B **76**, 085341 (2007).
[8] F. Cavaliere, U. D. Giovannini, M. Sassetti, and B. Kramer, New J. Phys. **11**, 123004 (2009).
[9] C. Ellenberger, T. Ihn, C. Yannouleas, U. Landman, K. Ensslin, D. Driscoll, and A. C. Gossard, Phys. Rev. Lett. **96**, 126806 (2006).
[10] O. M. Auslaender, H. Steinberg, A. Yacoby, Y. Tserkovnyak, B. I. Halperin, K. W. Baldwin, L. N.Pfeiffer, and K. W. West, Science **308**, 88 (2005).

[11]L. H. Kristinsdottir, J. C. Cremon, H. A. Nilsson, H. Q. Xu, L. Samuelson, H. Linke, A. Wacker, and S. M. Reimann, Phys. Rev. B **83**, 041101 (2011).
[12]N. Traverso Ziani, F. Cavaliere, and M. Sassetti, Phys. Rev. B **86**, 125451 (2012).
[13]V. V. Deshpande and M. Bockrath, Nat. Phys. **4**, 314 (2008).
[14]A. Secchi and M. Rontani, Phys. Rev. B **82**, 035417 (2010).
[15]A. Secchi and M.Rontani, Phys. Rev. B **85**, 121410 (2012).
[16]V. V. Deshpande, M. Bockrath, L. I. Glazman, and A. Yacoby, Nature (London) **464**, 209 (2010).
[17]J. M. Taylor and T. Calarco, Phys. Rev. A **78**, 062331 (2008).
[18]A. Ghosal, A. D. Guclu, C. J. Umrigar, D. Ullmo, and H. U. Baranger, Nat. Phys. **2**, 336 (2006).
[19]A. D. Guclu, A. Ghosal, C. J. Umrigar, and H. U. Baranger, Phys. Rev. B **77**, 041301 (2008).
[20]L. Shulenburger, M. Casula, G. Senatore, and R. M. Martin, Phys. Rev. B **78**, 165303 (2008).
[21]E. M. Stoudenmire, L. O. Wagner, S. R. White, and K. Burke, Phys. Rev. Lett. **109**, 056402 (2012).
[22]P. Hohenberg and W. Kohn, Phys. Rev. **136**, B 864 (1964).
[23]W. Kohn and L. J. Sham, Phys. Rev. A **140**, 1133 (1965).
[24]V. I. Anisimov, J. Zaanen, and O. K. Andersen, Phys. Rev. B **44**, 943 (1991).
[25]M. Grüning, O. V. Gritsenko, and E. J. Baerends, J. Chem. Phys. **118**, 7183 (2003).
[26]A. J. Cohen, P. Mori-Sanchez, and W. T. Yang, Science **321**, 792 (2008).
[27]M. Borgh, M. Toreblad, M. Koskinen, M. Manninen, S. Aberg, and S. M. Reimann, Int. J. Quantum Chem. **105**, 817 (2005).
[28]S. H. Abedinpour, M. Polini, G. Xianlong, and M. P. Tosi, Eur. Phys. J. B **56**, 127 (2007).
[29]C. Verdozzi, Phys. Rev. Lett. **101**, 166401 (2008).
[30]N. Helbig, I. V. Tokatly, and A. Rubio, J. Chem. Phys. **131**, 224105 (2009).
[31]D. G. Tempel, T. J. Martínez, and N. T. Maitra, J. Chem. Theory Comput. **5**, 770 (2009).
[32]A. M. Teale, S. Coriani, and T. Helgaker, J. Chem. Phys. **130**, 104111 (2009).
[33]A. M. Teale, S. Coriani, and T. Helgaker, J. Chem. Phys. **132**, 164115 (2010).
[34]S. Kurth, G. Stefanucci, E. Khosravi, C. Verdozzi, and E. K. U. Gross, Phys. Rev. Lett. **104**, 236801 (2010).
[35]G. Stefanucci and S. Kurth, Phys. Rev. Lett. **107**, 216401 (2011).
[36]A. Takayama, T. Sato, S. Souma, and T. Takahashi, Phys. Rev. Lett. **106**, 166401 (2011).
[37]J. P. Bergfield, Z.-F. Liu, K. Burke, and C. A. Stafford, Phys. Rev. Lett. **108**, 066801 (2012).
[38]J. D. Ramsden and R. W. Godby, Phys. Rev. Lett. **109**, 036402 (2012).
[39]M. A. Buijse, E. J. Baerends, and J. G. Snijders, Phys. Rev. A **40**, 4190 (1989).
[40]C. Filippi, C. J. Umrigar, and M. Taut, J. Chem. Phys. **100**, 1290 (1994).
[41]O. V. Gritsenko, R. van Leeuwen, and E. J. Baerends, Phys. Rev. A **52**, 1870 (1995).
[42]O. V. Gritsenko, R. van Leeuwen, and E. J. Baerends, J. Chem. Phys. **104**, 8535 (1996).
[43]F. Colonna and A. Savin, J. Chem. Phys. **110**, 2828 (1999).
[44]P. Mori-Sanchez, A. J. Cohen, and W. T. Yang, Phys. Rev. Lett. **102**, 066403 (2009).
[45]D. Vieira, Phys. Rev. B **86**, 075132 (2012).
[46]A. J. Cohen, P. Mori-Sánchez, and W. Yang, Chem. Rev. **112**, 289 (2012).
[47]P. Gori-Giorgi, M. Seidl, and G. Vignale, Phys. Rev. Lett. **103**, 166402 (2009); Z. F. Liu and K. Burke, J. Chem. Phys. **131**, 124124 (2009).
[48]P. Gori-Giorgi and M. Seidl, Phys. Chem. Chem. Phys. **12**, 14405 (2010).
[49]F. Malet and P. Gori-Giorgi, Phys. Rev. Lett. **109**, 246402 (2012).
[50]M. Levy, Proc. Natl. Acad. Sci. USA **76**, 6062 (1979).
[51]D. C. Langreth and J. P. Perdew, Solid State Commun. **17**, 1425 (1975).
[52]O. Gunnarsson and B. I. Lundqvist, Phys. Rev. B **13**, 4274 (1976).
[53]M. Seidl, Phys. Rev. A **60**, 4387 (1999).
[54]M. Seidl, J. P. Perdew, and M. Levy, Phys. Rev. A **59**, 51 (1999).
[55]M. Seidl, J. P. Perdew, and S. Kurth, Phys. Rev. Lett. **84**, 5070 (2000).
[56]M. Seidl, P. Gori-Giorgi, and A. Savin, Phys. Rev. A **75**, 042511 (2007).
[57]E. Räsänen, M. Seidl, and P. Gori-Giorgi, Phys. Rev. B **83**, 195111 (2011).
[58]G. Buttazzo, L. De Pascale, and P. Gori-Giorgi, Phys. Rev. A **85**, 062502 (2012).
[59]P. Gori-Giorgi, G. Vignale, and M. Seidl, J. Chem. Theory Comput. **5**, 743 (2009).
[60]A. Mirtschink, M. Seidl, and P. Gori-Giorgi, J. Chem. Theory Comput. **8**, 3097 (2012).
[61]M. Levy and J. P. Perdew, Phys. Rev. A **32**, 2010 (1985).
[62]M. Seidl, J. P. Perdew, and S. Kurth, Phys. Rev. A **62**, 012502 (2000).
[63]S. Bednarek, B. Szafran, T. Chwiej, and J. Adamowski, Phys. Rev. B **68**, 045328 (2003).
[64]L. Calmels and A. Gold, Phys. Rev. B **56**, 1762 (1997).
[65]M. Rontani, C. Cavazzoni, D. Bellucci, and G. Goldoni, J. Chem. Phys. **124**, 124102 (2006).
[66]S. M. Reimann and M. Manninen, Rev. Mod. Phys. **74**, 1283 (2002).
[67]G. F. Giuliani and G. Vignale, *Quantum Theory of the Electron Liquid* (Cambridge University Press, New York, 2005).
[68]M. Casula, S. Sorella, and G. Senatore, Phys. Rev. B **74**, 245427 (2006).
[69]D. Vieira and K. Capelle, J. Chem. Theory Comput. **6**, 3319 (2010).
[70]D. Vieira, arXiv:1212.3241.
[71]C.-O. Almbladh and U. von Barth, Phys. Rev. B **31**, 3231 (1985).
[72]M. Levy, J. P. Perdew, and V. Sahni, Phys. Rev. A **30**, 2745 (1984).
[73]C. B. Mendl and L. Lin, Phys. Rev. B **87**, 125106 (2013).